Antimetabolite Drugs Exhibit Distinctive Immunomodulatory Mechanisms and Effects on the Intestinal Microbiota in Experimental Autoimmune Uveitis

Victor Llorenç,[1–3] Yukiko Nakamura,[3] Christina Metea,[3] Lisa Karstens,[3] Blanca Molins,[2] and Phoebe Lin[3]

[1]Clínic Institute of Ophthalmology (ICOF), Clínic Hospital of Barcelona, Barcelona, Spain
[2]Biomedical Research Institute August Pi i Sunyer (IDIBAPS), Clínic Hospital of Barcelona, Barcelona, Spain
[3]Casey Eye Institute, Oregon Health & Science University, Portland, Oregon, United States

Correspondence: Victor Llorenç, Clínic Institute of Ophthalmology, Clínic Hospital of Barcelona, Sabino de Arana str., 1, 2nd floor, PC 08028-Barcelona, Spain; llorens.victor@gmail.com.

Received: August 26, 2021
Accepted: March 8, 2022
Published: March 31, 2022

Citation: Llorenç V, Nakamura Y, Metea C, Karstens L, Molins B, Lin P. Antimetabolite drugs exhibit distinctive immunomodulatory mechanisms and effects on the intestinal microbiota in experimental autoimmune uveitis. *Invest Ophthalmol Vis Sci.* 2022;63(3):30. https://doi.org/10.1167/iovs.63.3.30

Purpose. The purpose of this study was to investigate the effect of antimetabolite drugs on T-cell responses and intestinal microbial composition in autoimmune uveitis.

Methods. Experimental autoimmune uveitis (EAU) was induced in C57BL/6J mice treated with 0.00625 mg/mL methotrexate (MTX) or 0.625 mg/mL mycophenolate mofetil (MMF) in drinking water for 4 weeks prior to immunization and 2 weeks thereafter. The effector T cell (Teff) and regulatory T cell (Treg) populations were identified using flow cytometry. The 16S rRNA gene sequencing was applied for gut microbiome characterization. DESeq2 analysis was used to discriminate relative abundances of taxa and PLS-DA to integrate cytometric and microbiome data between groups.

Results. Both MTX and MMF abrogated uveitis in EAU without clinical signs of toxicity as compared to water-fed controls. MTX reduced Teff and Treg expansion in peripheral tissues and eyes. MTX decreased alpha diversity, increased *Akkermansia*, and reduced *Lachnoclostridium* abundances. Conversely, MMF enhanced Tregs in the mesenteric lymph node and the eyes. In parallel, MMF increased the gut alpha diversity, including an increased abundance of *Lachnospiraceae* NK4A136 group and a decreased abundance of *Lachnospiraceae* UCG-001. A significant congruent correlation among intestinal microbial changes, T-cell responses, and clinical scores was observed for both antimetabolites.

Conclusions. Although MTX and MMF both abrogated uveitis in EAU, they showed different effects on T-cell subsets and the intestinal bacterial composition. This work indicates unique immunomodulation by each drug and is the first to demonstrate potential microbiota-related mechanisms.

Keywords: antimetabolites, experimental autoimmune uveitis, methotrexate, intestinal microbiome, mycophenolate mofetil, uveitis

Resumen

Objetivo. Investigar el efecto de los fármacos antimetabolitos sobre las respuestas de células T y la composición microbiana intestinal en la uveítis autoinmune.

Métodos. Se indujo uveítis autoinmune experimental (UAE) en ratones C57BL/6J tratados con 0.00625 mg/ml de metotrexato (MTX) o 0.625 mg/ml de micofenolato mofetilo (MFM) en agua de bebida durante 4 semanas antes de la inmunización y 2 semanas después. Las poblaciones de células T efectoras (Tef) y reguladoras (Treg) se identificaron por citometría de flujo. La caracterización del microbioma intestinal se realizó mediante secuenciación del gen 16S ARNr. El análisis discriminante de abundancias relativas en los taxones se llevó a cabo por DESeq2 y se usó un análisis PLS-DA para integrar los datos microbianos y citométricos entre grupos.

Resultados. MTX y MFM inhibieron la UAE sin signos clínicos de toxicidad comparado con los controles. MTX disminuyó la expansión de Tef y Treg en los tejidos periféricos y oculares. MTX redujo la alfa diversidad, incrementando la abundancia de Akkermansia, y reduciendo la de Lachnoclostridium. En cambio, MFM aumentó los Tregs en el ganglio mesentérico y en los ojos. Paralelamente, MFM aumentó la alfa diversidad, incluyendo un aumento de la abundancia del grupo Lachnospiraceae NK4A136 y un descenso de la de Lachnospiraceae UCG-001. Se observó una correlación congruente significativa, para

iovs.arvojournals.org | ISSN: 1552-5783

ambos fármacos, entre los cambios en el microbioma, las respuestas de células T y los grados clínicos de uveítis.

Conclusiones. Aunque ambos, MTX y MFM, suprimieron la UAE, mostraron efectos diferentes sobre los subtipos de células T y sobre la composición del microbioma. Este estudio indica un efecto inmunomodulador único para cada fármaco y es el primero en demostrar potenciales mecanismos relacionados con el microbioma.

Uveitis remains a leading cause of visual disability worldwide. Around 20% of legal blindness has been attributed to uveitis.[1] Corticosteroids are still the standard of care treatment in noninfectious uveitis (NIU). Nevertheless, early initiation of immunomodulatory therapy in NIU has been proven to be beneficial for visual outcome and to avoid corticosteroid-related toxicity.[2]

The antimetabolite drugs, methotrexate (MTX) and mycophenolate mofetil (MMF), are the preferred first line immunomodulators by uveitis practitioners.[3] However, about 34% and 27% of patients fail to reach complete ocular inflammation control, and 42% and 45% do not reach an acceptable corticosteroid-sparing effect at 12 months of follow-up, with MTX and MMF, respectively.[4]

Cancer research shows that high dose MTX, an inhibitor of dihydrofolate reductase, is a strong cytotoxic drug that inhibits the synthesis of purines, inducing apoptosis in rapidly dividing malignant cells.[5] However, the anti-inflammatory mechanism at low doses for a long period of time, such as those used in NIU, is incompletely understood.[6] MMF exerts its cytotoxic effects as an inosine-5′-monophosphate dehydrogenase inhibitor, limiting the rate of de novo guanosine nucleotide synthesis, which is essential for the proliferation of activated T and B lymphocytes.[7] However, the intrinsic mechanisms by which MMF suppresses clinical inflammation at low doses are also unclear. Decreased nitric oxide (NO) production through NO synthase inhibition, reduction in cytokine production, as well as suppression of recruitment into the sites of inflammation; have been postulated as possible mechanisms.[8]

The intestinal microbiota has recently been investigated as a potential therapeutic target to achieve higher efficacy and lower toxicity of several chemotherapeutic drugs, including MTX.[9,10] Further research in experimental autoimmune uveitis (EAU) demonstrates a strong influence of the gut microbiome on the adaptive immune response and clinical severity of uveitis.[11,12]

In this study, we hypothesized that MTX and MMF induce unique intestinal microbial changes that could be correlated with specific mechanisms of T-cell modulation in EAU.

Methods

Mouse Treatments

Male 5- to 8-week-old C57BL/6J mice were purchased from Jackson Lab (Sacramento, CA, USA). Mice were maintained under conventional housing conditions, with HEPA-filtered cages and balanced irradiated chow ad libitum. The experimental protocols adhered to the ARVO Statement for the Use of Animals in Ophthalmic and Vision Research and were approved by the Oregon Health & Science University Institutional Animal Care and Use Committee. Ultrapure drinking water was prepared with a solution of MTX 0.00625 mg/mL (1 g powder/vial; Hikma, Thymoorgan Pharmazie GmbH, Germany) or MMF 0.625 mg/mL (500 mg powder/vial; CellCept; Hoffman-La Roche, Basel, Switzerland) in the treatment groups. Threshold for dehydration was set at <3 mL/mouse/day. A low-medium intake dose of MTX (0.80–1.00 mg/Kg body weight [BW]/day) and MMF (80–100 mg/Kg BW/day) was expected, as is typically used in the uveitis clinical setting, as described elsewhere.[7,13,14] Treatment with MTX or MMF started 4 weeks prior to immunization. Non-immunized controls, untreated and treated with MTX or MMF were included.

EAU Induction

Mice were immunized with 300 to 500 µg interphotoreceptor retinoid-binding protein (IRBP) 651 to 670 peptide (Genscript, Fremont, CA, USA) emulsified in Freund's adjuvant (Sigma-Aldrich Corp., St. Louis, MO, USA) containing 5 mg/mL heat-inactivated *Mycobacterium tuberculosis* (BD, Franklin Lakes, NJ, USA). Pertussis toxin (Sigma-Aldrich Corp.) was given subcutaneously, as previously described.[15,16] Clinical EAU score was evaluated by fundus examination at 1- and 2-weeks post-immunization.[17]

Cell Isolation

Without animal perfusion before euthanasia, single-cell suspensions were obtained by processing the spleen (SPN), mesenteric lymph node (MLN), and cervical lymph nodes (CLNs) through a 70 µm strainer. The lamina propria lymphocytes (LPLs) were isolated using 0.1 mg/mL collagenase II (Sigma-Aldrich Corp.) and 0.1 mg/mL DNase I (Roche, San Francisco, CA, USA) digestion and Percoll gradient according to previously published protocols.[18] Eyes were enucleated, the lens removed, and were minced. Eye pieces (2 eyes pooled from each mouse) were digested with 1 mg/mL collagenase D (Roche) and 15 µg/mL DNase I (Roche) at 37°C for 40 minutes and passed through a 70 µm strainer.

Flow Cytometry

The regulatory T-cell (Treg) panel included: CD4-FITC antibody (clone RM4-5), Live/Dead dye-efluor780 (eBioScience, San Diego, CA, USA) used after Fc blocking with rat anti-mouse CD16/CD32 Fc block (BD Pharmingen, San Jose, CA, USA), FoxP3-APC (clone FJK-16s), Helios-efluor450 (clone 22F6) (eBioScience) antibodies. For effector T-cells (Teff), single-cell suspensions were stimulated in vitro for 3 hours at 37°C with 500 ng/mL phorbol 12-myristate 13-acetate (PMA; Sigma-Aldrich Corp.) and 2 mg/mL ionomycin (Sigma-Aldrich Corp.) in culture media (10% FBS, RPMI, penicillin, streptomycin, and β-mercaptoethanol) in the presence of monensin (BD Biosciences, San Jose,

Investigative Ophthalmology & Visual Science

CA, USA). Cells were stained with CD4-PE-Cy7 (clone GK1.5; eBioscience/Affymetrix) and Live/Dead stain, then fixed and permeabilized using an intracellular cytokine detection kit (BD Biosciences). The intracellular staining panel included IFNγ-FITC (clone XMG1.2; BD Biosciences), TNF-α -phycoerythrin (TNF-α -PE; clone TN3-19.12; eBioscience/Affymetrix), IL-2-Alexa Fluor 700 (IL-2-AF700; clone JES6-5H4), and IL-17A Alexa Fluor 647 (IL-17A-AF647; clone TC11-18H10; BD Pharmingen). Flow cytometric data were acquired on a LSRFortessa cell analyzer (BD Biosciences). Samples not reaching a minimum of 1000 live cell counts for eyes and 2000 live cell counts for other tissues, and those with abnormal flow plot patterns, in a double-step quality data assessment, were excluded from analysis. Along with relative T-cell subsets, absolute counts were also compared due to significant immunosuppression caused by MTX, assuming similar average in tissue volumes and processing methods among groups.

The 16S rRNA Gene Sequencing

Cecal contents were collected in sterile conditions under laminar flow hood and stored at −20°C until DNA isolation (DNeasy PowerSoil, Quiagen, Germany). Amplification of the 16S rRNA gene was performed using standard protocols of the Earth Microbiome Project (www.earthmicrobiome.org).[19] The V4 region of the 16S gene was targeted with universal primers 515-F/806RB and sequenced with the Illumina MiSeq. The Divisive Amplicon Denoising Algorithm (DADA2) in R was implemented to find unique phylogenetic units. The DADA algorithm denoises and demultiplexes 16S sequences into distinct sequences called amplicon sequence variants (ASVs).[20] Phylogenetic identification was performed by aligning the ASVs to the SILVA version 132 16S rRNA database (https://www.arb-silva.de/). Alpha diversity and beta diversity measures were calculated using the VEGAN and phyloseq packages in R software.[21] The phylogenetic tree used for the UNIFRAC calculation was created using the R DECIPHER package.[22] The UNIFRAC distances were also used to test for significant differences using the PERMANOVA test using 1000 permutations. To identify differentially abundant taxa between groups for those taxa found at more than 0.2% of total abundance and represented in at least 10% of samples, we utilized DESeq2 to detect significant differential expression based on generalized linear models.[18,23]

Luminex Cytokine Quantification

Supernatants were obtained from stimulated single-cell suspensions (SPN, MLN, CLN, LPL, and EYE), and stored at −80°C until the Luminex assay (Life Technologies) was performed, after which cytokine production was quantified through a Luminex 200 analyzer (Luminex Corp., Austin, TX, USA).

Ileum Morphology

Paraffin-embedded ileal tissue was sectioned, stained with hematoxylin and eosin, then photographed using a DM5000 B microscope, DC500 camera, and IM50 software (Leica, Wetzlar, Germany). Three ileum sections from each animal were measured: villus and crypt length, and submucosa and muscularis thickness, in two non-contiguous different areas, using ImageJ.[24]

Quantitative Reverse-Transcriptase PCR

Fresh ileum tissue was snap-frozen and stored at −80°C until RNA isolation. The RNA was extracted with TRIzol (Life Technologies), and cDNA synthesized at 37°C using a cDNA synthesis kit (Thermo Applied Biosystems). Gene expression of anti-microbial peptides (AMPs) and various cytokines were quantified using previously reported custom-made primer sets.[16] Real-time (RT)-PCR was performed using SYBR Green reagents (Quanta Biosciences, Beverly, MA, USA) on a ViiA 7 Real-time PCR machine (Thermo Fisher Scientific). Relative expression of these target genes compared to internal controls (HPRT or GAPDH) was calculated.

Statistical Analyses

Data are expressed as mean ± standard deviation (SD). Mann-Whitney U tests were performed for comparisons using GraphPad Prism 7 (GraphPad Software, Inc., La Jolla, CA). Partial Least Squares Discriminant-Analysis (PLS-DA), which combines a reduction through Principal Components Analysis followed by logistic regression was conducted with cytometric and microbiological covariates. PLS-DA was performed with XLStat software (XLStat versopm 2014.1.01; Addinsoft, France). The bacterial taxa used in the PLS-DA were also those that comprised at least 0.2% of total abundance and 10% prevalence among all samples (as stated above for the DESeq). Clinical score at 2 weeks was used as an internal reference control. A threshold of $P < 0.05$ was considered statistically significant.

Results

Monitoring Body Weight, Water, and Drug Intake

There were no signs or symptoms of toxicity in any group during the study period. The BW gain was 5.49 ± 2.03 g, 4.14 ± 1.34 g, and 6.70 ± 2.76 g in the water, MTX, and MMF groups, respectively, without significant differences. Water intake was higher in the control group (5.41 ± 0.59 mL/mouse/day) than in the MTX (4.56 ± 0.33 mL/mouse/day; $P < 0.0001$) and MMF (4.27 ± 0.56 mL/mouse/day; $P < 0.0001$) groups. All groups experienced a significant reduction in water intake in the days following immunization compared to baseline. However, no group was under the threshold for dehydration (<3 mL/mouse/day) at any point. Drug intake was 1.15 ± 0.08 mg/Kg BW/mouse/day for MTX and 106.80 ± 13.98 mg/Kg BW/mouse/day for MMF group. Cumulative doses of MTX and MMF at the euthanasia point were 7.11 mg/Kg BW and 643.3 mg/Kg BW, respectively (See Supplementary Material Fig. S1 for sequential drug and water intake).

EAU Clinical Score

At 1-week post-immunization, all animals scored 0+ to 0.5+ in the EAU clinical score, without differences between groups. At 2 weeks, mean clinical score in the control group peaked at 1.59 ± 0.91 compared with MTX (0.30 ± 0.11; $P < 0.0001$), and MMF (0.25 ± 0.29; $P < 0.0001$; Fig. 1). Anterior segment signs of inflammation were more frequent in the control group (posterior synechiae 38.88% and limbal injection 25.92% of the eyes) than in the

Investigative Ophthalmology & Visual Science

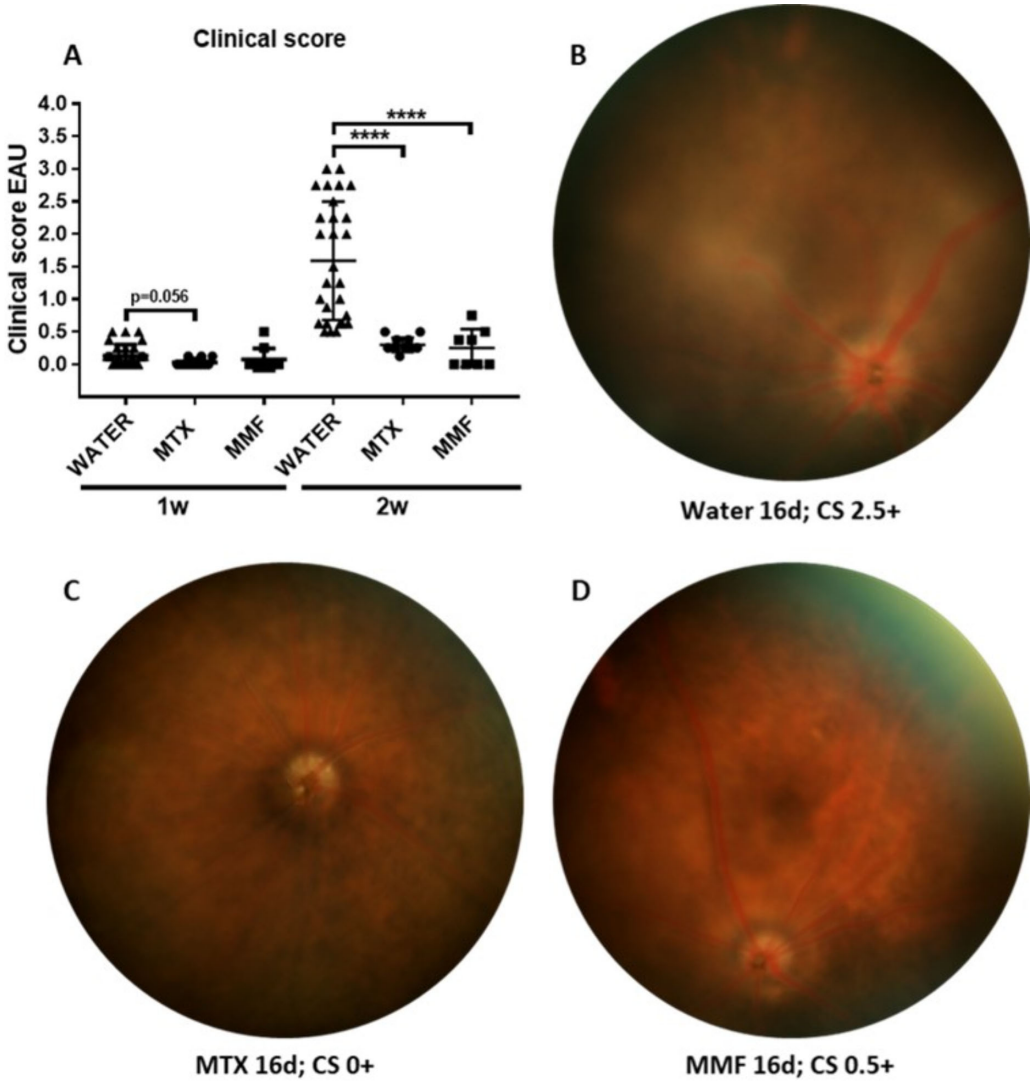

Figure 1. Differences in clinical score among control (water), methotrexate (MTX) and mycophenolate mofetil (MMF) groups in experimental autoimmune uveitis (EAU). (**A**) Differences in the EAU clinical score among groups at 1 and 2 weeks; examples of fundus photos of (**B**) water (control group); (**C**) MTX-treated EAU mice; and (**D**) MMF-treated mice. w, weeks post-immunization; d, days post-immunization; CS, clinical score. ****$P < 0.0001$. Data expressed as mean ± standard deviation, $n = 8$ to 26 mice per group.

MTX (posterior synechiae 0.00%; $P = 0.0001$ and limbal injection 0.00%; $P = 0.004$), and MMF group (posterior synechiae 0.00%; $P = 0.002$ and limbal injection 12.50%; $P = 0.329$).

Treg and Teff Modulation by MTX and MMF

Absolute counts of CD_4^+ $Foxp3^+$ (Tregs) as well as CD_4^+ $Foxp3^+$ $Helios^+$ (He^+) subpopulations were decreased in the eyes, LPL, and MLN in MTX-treated EAU mice, as compared to controls and MMF. Conversely, CD_4^+ $Foxp3^+$ and CD_4^+ $Foxp3^+$ He^+ were enhanced in the MLN of MMF-treated animals. The absolute counts of Teff (shown are CD4+, IFNγ+, IL17A+, TNFα+, and IL-2+) were significantly reduced in the eyes and other lymphoid tissues in the MTX group. Teff subpopulations were increased rather than decreased in the MLN of animals treated with MMF (Fig. 2). The proportion of Teff was higher among the scarce absolute number of lymphocytes remaining in the eyes of MTX treated animals. Interestingly, the proportion of He^+ among CD_4^+ $Foxp3^+$ lymphocytes was increased in the eyes, MLN, and SPN of those animals treated with MMF (Figs. 3, 4, 5). In non-immunized controls, no significant differences were found among water-fed, MTX, and MMF treated mice for any Treg nor Teff lymphocyte subset in any tissue, either absolute or relative cell counts.

Gut Microbial Changes Induced by MTX and MMF

In EAU, a significant difference in beta diversity was observed after treatment with MTX and MMF as compared to controls. A PERMANOVA on the weighted UniFrac analysis was significant between MTX and H_2O ($P = 0.009$), as well as between MMF and H_2O ($P = 0.019$). There was a significant alpha biodiversity change after treatment with MTX and MMF, but in opposite directions. Although animals treated with MTX showed a decreased Shannon index, it was significantly enhanced with MMF. The same trend was observed for other alpha diversity indices. Furthermore, there was a reduced Firmicutes/Bacteroidetes ratio (F/B) with MTX

Investigative Ophthalmology & Visual Science

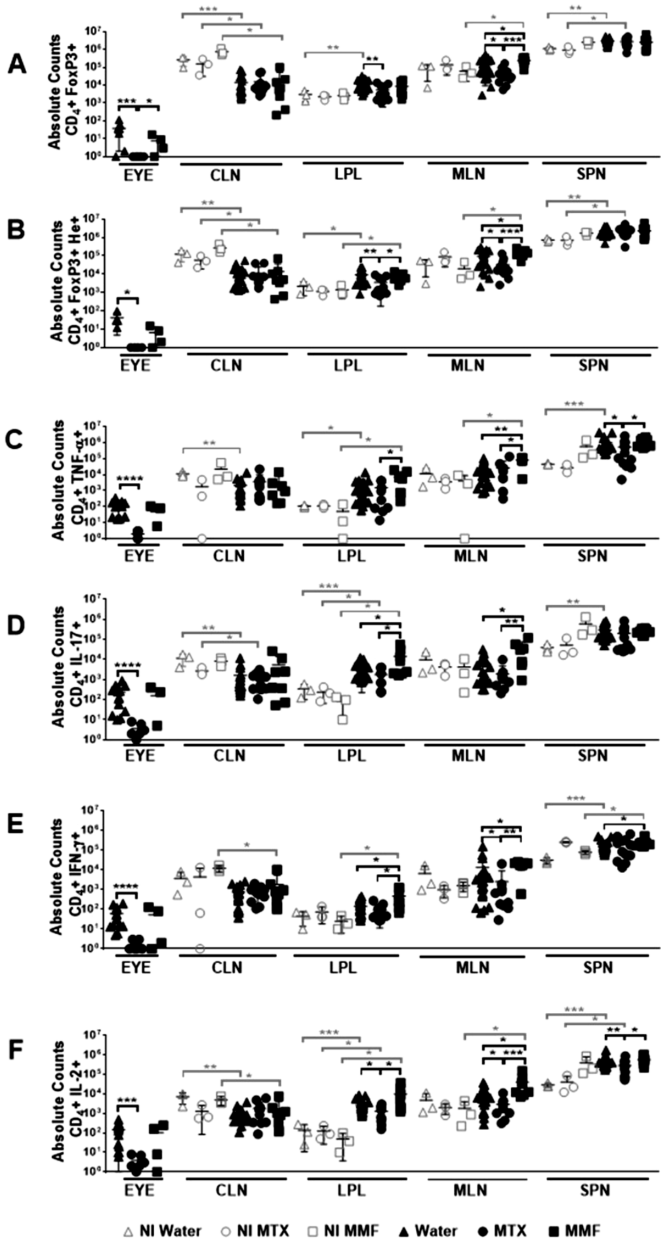

Figure 2. Absolute counts of T regulatory (**A, B**) and T effector (**C, D, E, F**) lymphocyte subpopulations in different tissues after antimetabolite treatment in experimental autoimmune uveitis and non-immunized controls. CLN, cervical lymph nodes; LPL, gut lamina propria; MLN, mesenteric lymph node; SPN, spleen; NI, non-immunized; Water, control group; MTX, methotrexate treated mice; MMF, mofetil mycophenolate treated mice. *$P < 0.05$, **$P < 0.01$, ***$P < 0.001$, ****$P < 0.0001$. Data expressed as mean ± standard deviation; $n = 3$ mice per group (non-immunized), and 5 to 20 mice per group (immunized). Time-point = 6 weeks post-treatment initiation, 2 weeks post-immunization.

(H_2O F/B = 2.03 ± 0.85 versus MTX F/B = 1.49 ± 0.53; $P = 0.031$), whereas it was increased after MMF treatment as compared to controls (MMF F/B = 3.12 ± 1.38; $P = 0.018$) and MTX ($P = 0.006$). No significant differences in beta diversity (NI water versus NI MTX, $P = 0.209$; NI water versus NI MMF, $P = 0.125$) and in alpha diversity were found among non-immunized animals, treated, or water-fed (Fig. 6).

Significant changes in relative abundance of certain bacterial genera were found with MTX and MMF. MTX induced increased relative abundance of *Faecalibaculum*, *Akkermansia*, and *Bacteroides,* among other genera, in EAU mice. Conversely, the relative abundance of the *Lachnoclostridium*, *Firmicutes* GCA-900066575, and *Lachnospiraceae* FCS020 groups, were reduced.

On the other hand, EAU mice treated with MMF showed a decreased relative abundance in *Lachnospiraceae* UCG-001 (Fig. 7). This effect was also observed in non-immunized mice treated with MMF (see Supplementary Material Fig. S2 for differential abundance data in non-immunized controls).

Integrative Statistical Analysis

In a PLS-DA analysis, the highest discriminant covariates between the EAU water-fed controls and the MTX group

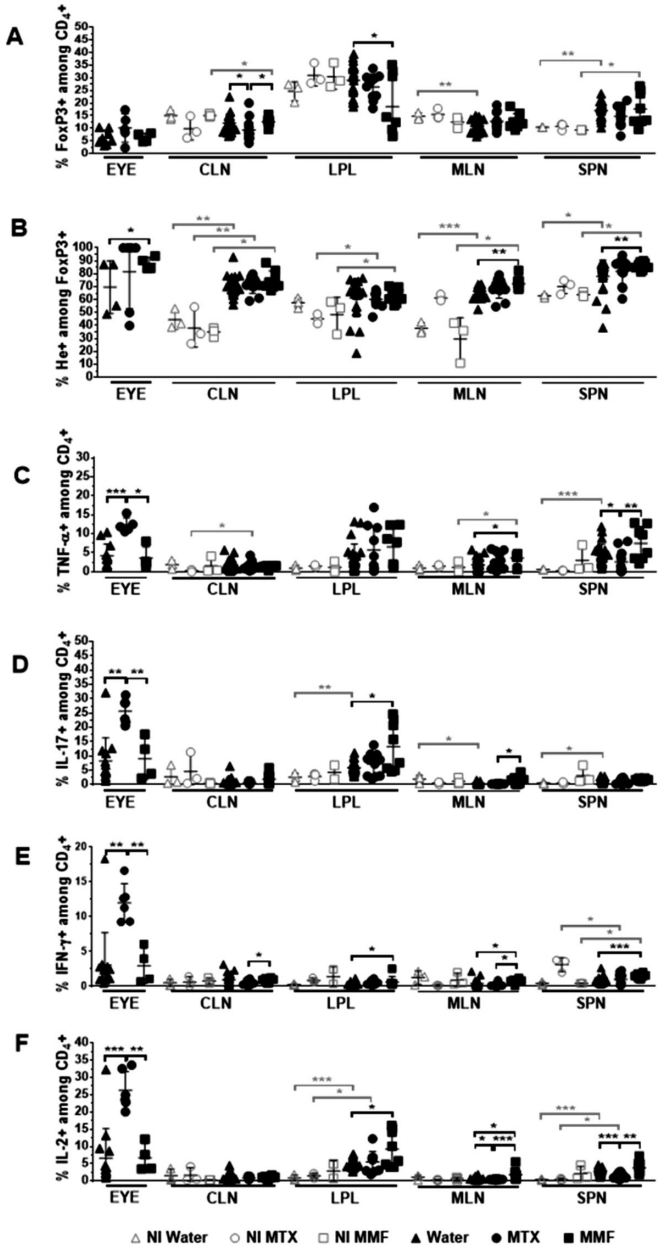

Figure 3. Relative counts of T regulatory (**A, B**) and T effector (**C, D, E, F**) lymphocyte subpopulations in different tissues after antimetabolite treatment in experimental autoimmune uveitis and non-immunized controls. CLN, cervical lymph nodes; LPL, gut lamina propria; MLN, mesenteric lymph node; SPN, spleen; NI, non-immunized; Water, control group; MTX, methotrexate treated mice; MMF, mofetil mycophenolate treated mice. *$P < 0.05$, **$P < 0.01$, ***$P < 0.001$, ****$P < 0.0001$. Data expressed as mean ± standard deviation; $n = 3$ mice per group (non-immunized), and 5 to 20 mice per group (immunized). Time-point = 6 weeks post-treatment initiation, 2 weeks post-immunization.

were the absolute counts of CD_4^+ $Foxp3^+$ and $CD4^+$ TNF-α^+ lymphocyte subpopulations in the eyes, and the relative abundance of certain bacteria (*Lachnoclostridium* and *GCA_900066575*), all of which were depleted in the MTX-treated animals. Conversely, MTX treatment was associated with enhanced proportions of TNF-α^+ and IL-17^+ CD_4^+ lymphocytes in eyes, as well as the increased relative abundance of *Akkermansia*. Clinical score was included as a positive control in the PLS-DA and higher score was expectedly associated with the control (water) group. There was a strong positive correlation between the relative abundance of *Lachnoclostridium* and the absolute counts of CD_4^+ TNF-α^+ lymphocytes in the eye (r = 0.73, 95% confidence interval [CI] = 0.49 to 0.87; $P < 0.0001$) along with higher clinical score at 2 weeks (r = 0.61, 95% CI = 0.32 to 0.80; $P = 0.0001$) in pooled controls and MTX EAU animals.

In MMF-treated EAU mice, the proportion of He^+ CD_4^+ $Foxp3^+$ (Tregs) in the eye and the relative abundance of *Lachnospiraceae* NK4A136 group were among the most discriminant covariates, both of which were significantly enhanced in the MMF group (Fig. 8). In the pooled EAU controls and MMF group, the abundance of *Lachnospiraceae* NK4A136 was positively correlated with the proportion of He^+ CD_4^+ $Foxp3^+$ in the eyes (r = 0.43, 95% CI = 0.08 to 0.69; $P = 0.016$). Conversely, it was negatively correlated with the clinical score at 2 weeks (r = −0.60, 95% CI =

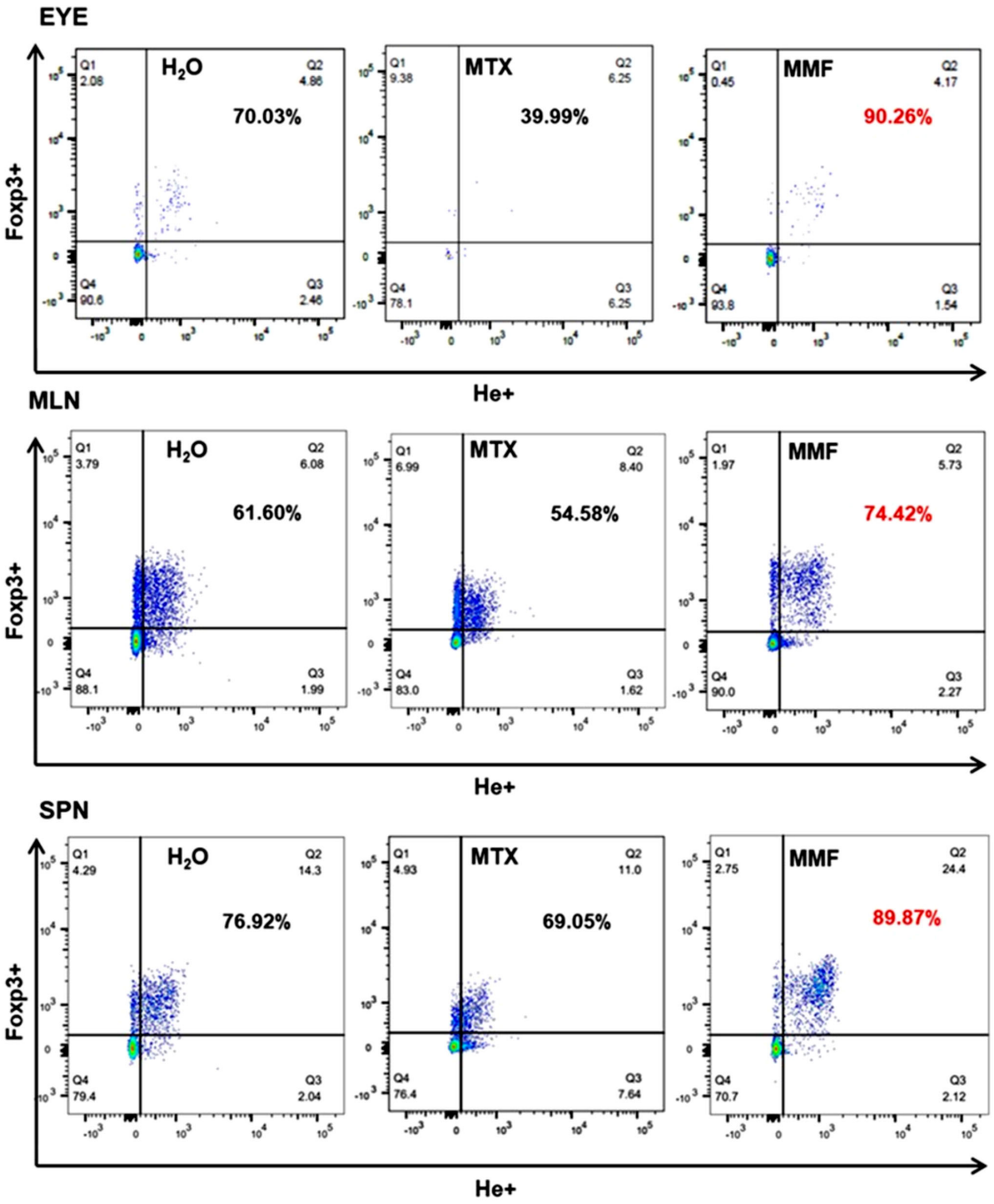

Figure 4. Rate of Helios$^+$ T regulatory lymphocyte subpopulations in representative tissues. Percentages refer to CD_4^+ Foxp3$^+$ He$^+$ life lymphocytes (Q2) among CD_4^+ Foxp3$^+$ life lymphocytes (Q1 + Q2). MLN, mesenteric lymph node; SPN, spleen; H_2O, water-fed control group; MTX, methotrexate treated mice; MMF, mofetil mycophenolate treated and immunized (experimental autoimmune uveitis) mice. Time-point = 2 weeks post-immunization.

−0.80 to −0.28; $P = 0.001$) and the absolute count of CD_4^+ TNF-α^+ lymphocytes in the eye (r = −0.78, 95% CI = −0.90 to −0.55; $P < 0.0001$).

Cytokine Release From CD_4^+ Stimulated Lymphocytes

In the EAU MTX group, there was a significant decrease in TNF-α, IL-17A, and IL-1β in eye tissue, as well as a decreased level of TNF-α, IL-1β, and IL-2 in LPL. Conversely, TNF-α, IL-17A, and IL-6 concentrations were significantly increased in the spleen and MLN tissues with MTX. In the MMF treated mice, a decreased level of IL-17A was found in the CLN (see Supplementary Material Table S1 for cytokine release in different tissues).

Ileum Histopathology

To investigate if MTX or MMF induced structural intestinal changes due to immunological or toxic effects, we

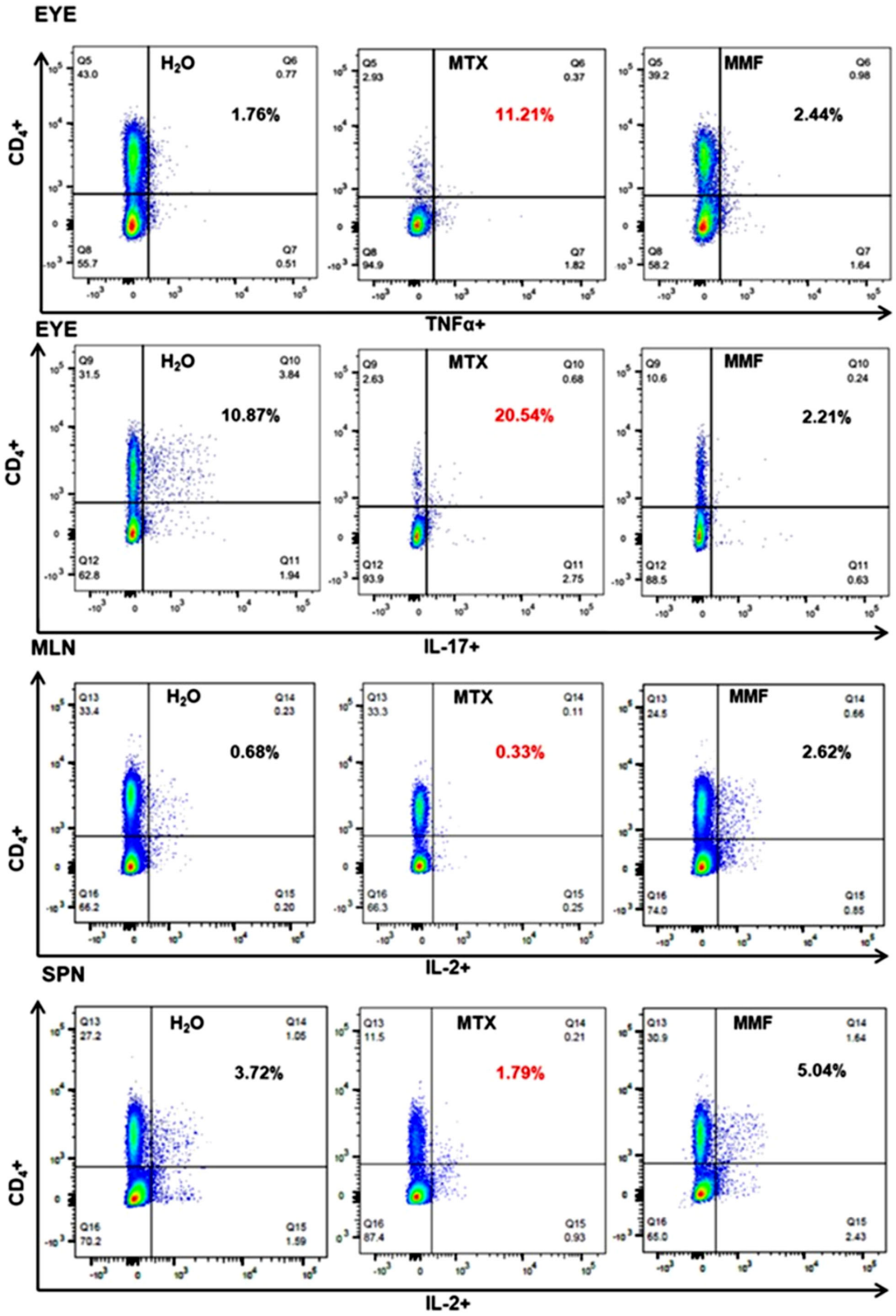

Figure 5. Rate of T effector lymphocyte subpopulations in representative tissues. Percentages refer to CD_4^+ $TNF\alpha^+$/IL-17^+/IL-2^+ life lymphocytes (Q2) among CD_4^+ life lymphocytes (Q1 + Q2). LPL, gut lamina propria; MLN, mesenteric lymph node; H_2O, water-fed control group; MTX, methotrexate treated mice; MMF, mycophenolate mofetil treated and immunized (experimental autoimmune uveitis) mice. Time-point = 2 weeks post-immunization.

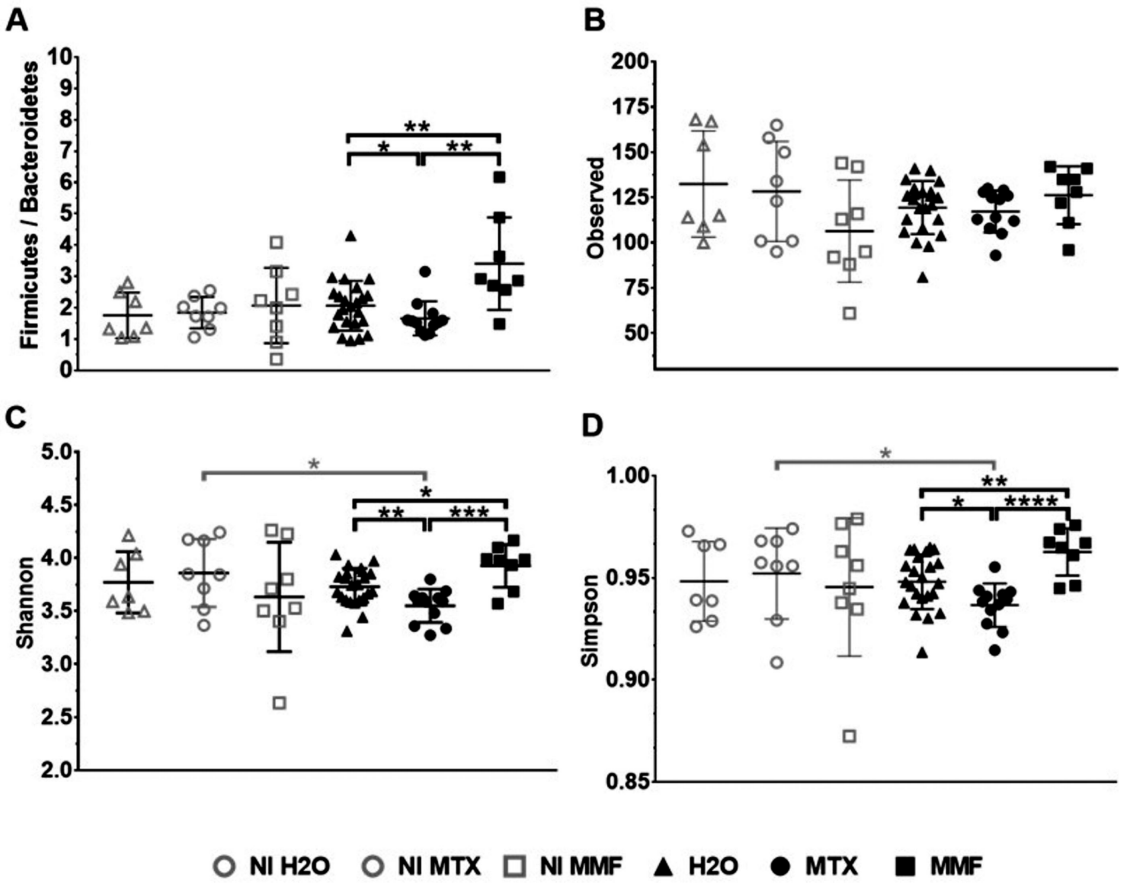

Figure 6. Alpha biodiversity indices after treatment with methotrexate (MTX) and mycophenolate mofetil (MMF) in immunized (experimental autoimmune uveitis) and non-immunized controls. Firmicutes/Bacteroidetes ratio (**A**), observed taxonomic units (**B**), Shannon index (**C**), and Simpson index (**D**). H_2O, water-fed. *$P < 0.05$, **$P < 0.01$, ***$P < 0.001$, ****$P < 0.0001$. Data expressed as mean ± standard deviation; $n = 7$ to 8 mice per group (non-immunized), and 8 to 20 mice per group (immunized). Time-point = 6 weeks post-treatment initiation, 2 weeks post-immunization.

performed ileum histopathology. A significant decrease in the submucosa thickness in the EAU MTX group (11.13 ± 3.25 µm versus control = 13.31 ± 2.87 µm; $P = 0.049$) and a significant increase in crypt length in the EAU MMF group (92.71 ± 18.96 µm versus control = 78.17 ± 11.31 µm; $P = 0.014$) was found. In non-immunized animals, MTX-treated mice showed a significant thinner submucosa than water-fed animals as well (NI water = 14.95 ± 3.22 µm versus NI MTX = 10.88 ± 0.86 µm; $P = 0.025$; see Supplementary Material Fig. S3 for histopathology changes). We have previously shown that subclinical intestinal inflammation and increased gut permeability occurs in EAU. Although we did not investigate gut permeability in this study, MTX and MMF may further exacerbate subclinical intestinal inflammation in EAU. Indeed, this side effect has been observed when given at higher doses for cancer treatment.[5,7,12] Ileal inflammation may be accompanied by structural changes other than increased length or thickness. For example, inflammatory conditions in the ileum may lead to crypt elongation, villi apex erosion, shortening and bleeding. Irregular crypt branching is also described as a sign of nonspecific inflammatory processes in the gut. Although the pathophysiological mechanism for this phenomenon is not well understood, it could be due to compensation to inflammatory damage.[25] Furthermore, in experimental autoimmune encephalomyelitis, the ileal submucosa becomes thickened, as presented by Nouri and colleagues.[26] In EAU and non-immunized C57Bl/6J mice, we did not observe microscopic hemorrhage, crypt branching, or any gross intestinal abnormalities in the treatment groups. However, our findings suggest that MMF likely causes some compensatory gut changes to localized subclinical inflammation by increasing crypt depth in EAU animals. The effect of MTX causing thinning of the submucosa could mean that it immunosuppresses the immunologically active sites in the gut, resulting in depletion of the leukocytes from this area resulting in submucosal hypoplasia.

Gene Expression in the Ileum

To assess putative antimetabolite effects on the expression of genes involved in host defense, including AMPs and cytokine production, RT-PCR in ileum tissue was performed. Microenvironmental changes in the ileum could influence microbiome composition which, in turn, may modulate local T cell activation or tolerance, migration to the target tissue, and subsequent ocular inflammation in EAU, as previously reported.[16] Trefoil factor 3 (TFF3) is a peptide secreted by mucin-producing intestinal goblet cells, promoting protection and repair. TFF3-deficient mice are vulnerable

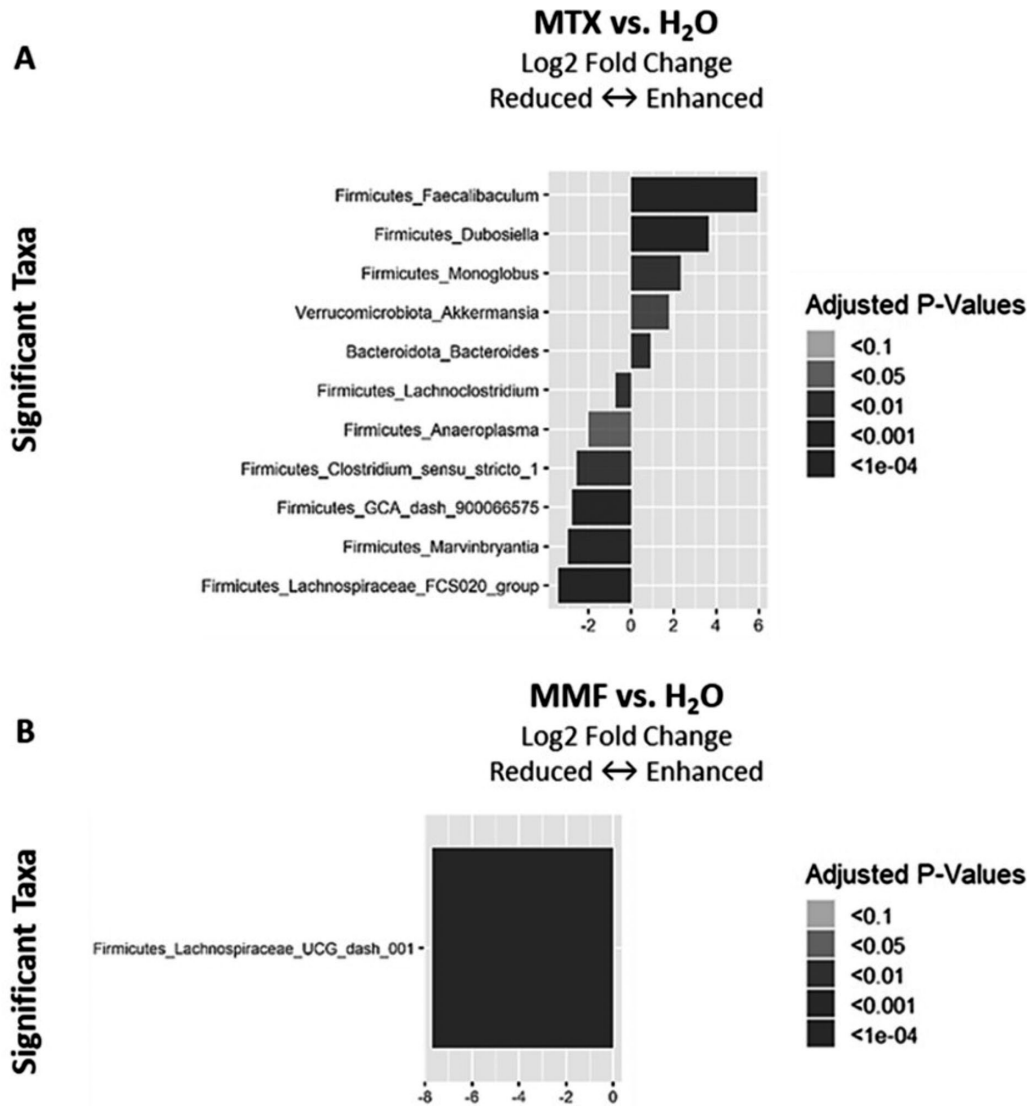

Figure 7. Differential abundances of intestinal bacterial genera in experimental autoimmune uveitis mice treated with methotrexate (MTX) (**A**) or mycophenolate mofetil (MMF) (**B**) as compared to water-fed (H_2O). Time-point = 6 weeks post-treatment initiation, 2 weeks post-immunization.

to dextran sulfate sodium-induced colitis, whereas administering TFF-3 promotes intestinal barrier function. AMPs, including regenerating islet-derived protein 3 gamma (Reg3) and calgranulin A (S100A8) are secreted by Paneth cells located at the bottom of the crypt, exert lytic, phagocytic, chemotactic activities, and are important in the clearance of endotoxins, such as bacterial lipopolysaccharide.[16,27] The EAU MMF-treated group expressed lower TFF3 than controls (MMF = 44.09 ± 16.3 versus water = 65.85 ± 25.39; P = 0.027). Relative expression of Reg3 and S100A8 were not significantly different among EAU groups. Relative expression of IFNγ in ileum was enhanced in the MMF-treated EAU mice as compared with either water (MMF = $38.05 \times 10^{-5} \pm 63.88 \times 10^{-5}$ versus water = $7.61 \times 10^{-5} \pm 12.47 \times 10^{-5}$; P = 0.024) or MTX-treated animals (versus MTX = $6.09 \times 10^{-5} \pm 7.16 \times 10^{-5}$; P = 0.032). There were no differences in IL-17 and IL-10 expression among EAU groups. These findings suggest that MMF may to some degree cause subclinical gut inflammation as a side effect due to downregulation of TFF3 expression (decreasing intestinal barrier function) as well as increasing the inflammatory cytokine IFNγ. Moreover, this is in accordance with the crypt enlargement by MMF (in the EAU mice) that may also suggest subclinical gut inflammation (see Supplementary Material Fig. S4 for relative gene expression in the ileum).

Discussion

In this work, both oral MTX and MMF abrogated uveitis in mouse EAU. Nevertheless, their mechanism on T lymphocyte response showed significant differences. Furthermore, MTX and MMF induced significant but disparate changes in the composition of the gut bacterial microbiome.

In EAU, MTX at low sustained doses, resulted in a significant suppressive effect of both Teff and Treg subpopulations in most tissues. Interestingly, although MTX reduced the absolute counts of CD_4^+ T-cells in eyes to a minimum, the proportion of Teff still residing in the target tissue was significantly higher than in controls and MMF-treated mice. This surprising finding may elicit a higher risk of relapse

Investigative Ophthalmology & Visual Science

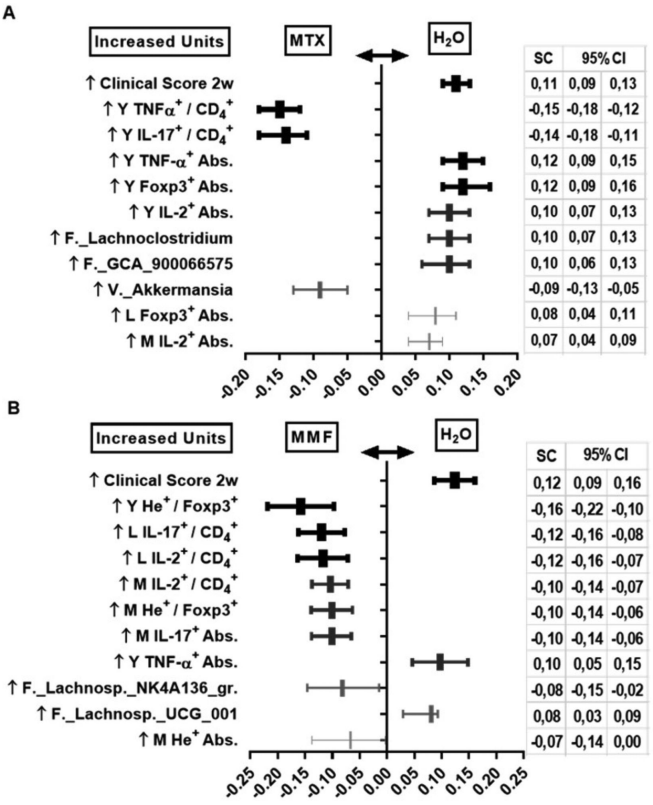

Figure 8. Partial least-squares discriminant analysis (PLS-DA) in immunized (experimental autoimmune uveitis) mice. Results between water-fed and methotrexate-treated (**A**), and between water-fed and mycophenolate mofetil-treated (**B**) animals. Only the 10 covariates with highest standardized scores (SC) plus reference control are shown, all $P < 0.05$. MTX, methotrexate; MMF, mycophenolate mofetil; H_2O, water-fed controls; w, weeks; Y, eye; L, gut lamina propria; M, mesenteric lymph node; Abs., absolute CD_4^+ lymphocyte counts. Time-point = 6 weeks post-treatment initiation, 2 weeks post-immunization.

after MTX cessation. In fact, Hiraoka et al. described a full-blown uveitis rebound one week after MTX cessation in Lewis rats.[14] We did not stop treatments to evaluate rebound in our model.

On the other hand, MMF-treated EAU mice showed increased absolute counts of CD_4^+ $Foxp3^+$ and CD_4^+ $Foxp3^+$ He^+ in the MLN as compared to water-fed controls or MTX. Furthermore, the proportion of $Foxp3^+$ CD_4^+ T-cells was higher in the CLN with MMF. MMF also increased the frequency of CD_4^+ $Foxp3^+$ He^+ lymphocytes in the eyes, MLN, and SPN. Treg lymphocytes expressing Helios show a more highly activated phenotype, are more suppressive, and have more stable Foxp3 expression than Helios negative T-regs.[28] They are highly effective in suppressing the immune response and inducing tolerance compared to Helios defective Tregs.[29] Moreover, several authors have demonstrated the pivotal role of He^+ Treg in maintaining inflammation quiescence in some immune-mediated diseases and its strong suppressive capability.[30] Therefore, whereas MTX seems to induce quiescence by suppressing Teff subsets, MMF may function partially through upregulation of regulatory T-cells.

Detection of proinflammatory cytokines in supernatants of stimulated cells corroborated a low effect of MMF but a suppressive cytokine release effect of MTX in eyes, CLN and LPL. However, a paradoxical increase of TNF-α, IL-17, and IL-6 in SPN and MLN with MTX suggests a possible role of other immune cell types, aside from CD_4^+ T lymphocytes, as previously suggested.[5,6]

In parallel, we found substantial intestinal microbial changes after MTX and MMF treatment in EAU. Interestingly, although MTX reduced alpha diversity, it depleted *Lachnoclostridium* and *GCA-900066575*, both of which were positively correlated with CD_4^+ TNF-α^+ lymphocytes absolute counts in the eyes and higher clinical uveitis score, suggesting that these MTX-induced intestinal microbial changes could be protective against uveitis. *Lachnoclostridium* and *GCA-900066575* may suppress growth of beneficial short chain fatty acid-producing bacteria.[31] Moreover, their relative abundances are increased in obese rodent models, linked to metabolic disorder[32–34] and colon cancer.[35,36]

MTX enhanced *Akkermansia* abundance, which correlated negatively with absolute counts of CD_4^+ TNF-α^+ lymphocytes in the eyes ($r = -0.37$; $P = 0.03$) and higher uveitis score ($r = -0.42$; $P = 0.013$). *Akkermansia* is depleted in B10.RIII mice after induction of EAU.[37] Interestingly, *Akkermansia* has shown key beneficial effects on several cardio-metabolic and inflammatory diseases by reducing systemic and local inflammation markers and restoring gut barrier integrity and has been postulated as a promising probiotic candidate.[38–40]

Furthermore, MMF treatment in EAU enhanced richness and evenness (alpha diversity) of bacterial genera overall. PLS-DA analysis revealed a negative association of *Lachnospiraceae* NK4A136, with CD_4^+ TNF-α^+ lymphocytes in eyes and clinical uveitis score, but positive correlation with He^+ $Foxp3^+$ T-cell percentage in the eyes, suggesting microbial changes that might contribute to immune regulation. Conversely, *Lachnospiraceae* UCG-001 was depleted by MMF in both, immunized and non-immunized animals. *Lachnospiraceae* comprises a varied group of genera with controversial and differential functions. In general, *Lachnospiraceae* has been found to be hyperabundant in metabolic syndrome, diabetes mellitus, and neuro-psychiatric disorders.[41] However, some genera are among the most active producers of beneficial short chain fatty acids. In fact, *Lachnospiraceae* NK4A136, which was enhanced and highly related to MMF immune effects, has been proposed as a potent probiotic, because its abundance is reduced in high-fat diet obese mice and restored after a shift to a regular balanced diet or prebiotic interventions.[42,43] Moreover, deficiency in *Lachnospiraceae* NK4A136 has been found in patients with uveitis associated with Behcet's disease, as compared to patients with mucocutaneous or vascular involvement without uveitis.[44] An anti-inflammatory effect has been attributed to *Lachnospiraceae* NK4A136,[45] and its relative abundance decreased in immunologically disbalanced mice caused by cyclophosphamide.[34]

Changes in ileal crypts and submucosal layers correlate with disease states in EAU and other inflammatory conditions. We found a slight degree of ileum submucosal atrophy induced by MTX, which is in line with its immunosuppressive effect noted on the LPL. However, thinner submucosa was also observed in non-immunized mice treated with MTX, suggesting that the effect is not necessarily linked to an underlying hyperinflammatory status. MMF caused an increased crypt depth, reversing the post-immunization changes previously described in EAU.[16] Furthermore, MMF reduced the expression of TFF3 in the ileum of EAU mice,

a peptide that induces mucosal protection.[27] MMF-induced TFF3 downregulation and increased IFNγ gene expression as well as the observed crypt enlargement may be signs of subclinical gut inflammation as a side effect of MMF treatment. MMF-induced intestinal subclinical inflammation may be clinically perceived as a drug intolerance.

We have previously shown that intestinal histological, gene expression, T cell types, and microbial changes are associated with the uveitic state in the inducible EAU model. Here, we illustrate that some of these impactful intestinal changes can be influenced by and likely explain part of the mechanism of standard immunosuppressive treatment for uveitis. For example, whereas the uveitic state has been shown to be associated with decreases in crypt depth prior to peak inflammation in EAU,[37] this is reversed by MMF treatment. *Akkermansia*, which is protective for the intestinal epithelial barrier, is depleted in the uveitic state,[18] but is enhanced by MTX treatment. Moreover, there are multiple intestinal bacteria the abundance of which are affected by the antimetabolites tested in this study that correlated with protective T-cell profiles in the eyes and other lymphoid tissues in the body suggesting that microbial changes likely play a role in the mechanism that these drugs have on uveitis control, along with non-microbial mechanisms. In particular, some antimetabolite-induced microbial changes likely promote a balance toward Tregs and away from inflammatory T cell subsets. However, given that this study did not utilize monoassociation studies with the intestinal bacteria that were found to be highly associated with beneficial changes, the direct immunological effect of some of these bacteria are yet to be proven.

This work provided new insights on the mechanisms of the most used immunosuppressant drugs in uveitis with a novel potential link to the intestinal microbiome. However, there are noteworthy limitations: the EAU model does not necessarily reflect the mechanistic pathways of the varied etiologies of uveitis in patients. In fact, treatment to reach antimetabolite therapeutic effect starts after uveitis onset in humans, whereas by necessity, we required pretreatment to reach therapeutic efficacy prior to waning of intraocular inflammation naturally in the self-limited EAU model. Microbiome composition between species may vary widely. Moreover, alternative route of administration, subcutaneous for MTX in particular, could influence its effects on the intestinal microbiome, and the analysis of eye-specific T-cell responses. Reproducibility in other animal models and humans, or with other routes of administration are required to corroborate the results reported.

In summary, our work suggests that both MTX and MMF inhibit clinical EAU through distinctive modulation of T-cell responses. Although MTX exerts a highly generalized Teff suppression, MMF balances the immune response toward tolerance by promoting highly effective Tregs. In parallel, MTX decreased the gut microbial diversity, limiting *Lachnoclostridium* growth and promoting *Akkermansia* growth. Conversely, MMF enriched gut bacterial diversity, enhancing the expansion of the *Lachnospiraceae* NK4A136 which, in turn, correlates with its effects on the T-cell immune response.

Whether the above-mentioned intestinal microbial changes links are directly mechanistic, or merely an association remains to be determined. Additional experiments would be necessary to demonstrate causality. Our findings suggest a larger role than previously demonstrated for antimetabolite efficacy and mechanism, potentially occurring through intestinal microbial effects on immunomodulation.

Acknowledgments

The authors thank Mark Asquith posthumously for his scientific advice and partnership.

P.L. has been supported by a National Eye Institute Grant K08 EY022948, a Collins Medical Trust Grant, and a Research to Prevent Blindness Career Development Award (P.L.). This study was also supported by core grant P30 EY010572 from the National Institute of Health (Bethesda, MD) and by unrestricted departmental funding from Research to Prevent Blindness (New York, NY). P.L. is also the recipient of an Alcon Research Institute Young Investigator Award and OHSU Physician-Scientist award, as well as recipient of a Thome Foundation award.

Disclosure: **V. Llorenç**, Alimera (C); **Y. Nakamura**, None; **C. Metea**, None; **L. Karstens**, None; **B. Molins**, None; **P. Lin**, Alcon (G)

References

1. Rothova A, Suttorp-van Schulten MS, Frits Treffers W, Kijlstra A. Causes and frequency of blindness in patients with intraocular inflammatory disease. *Br J Ophthalmol*. 1996;80(4):332–336.
2. Jabs DA, Rosenbaum JT, Foster CS, et al. Guidelines for the use of immunosuppressive drugs in patients with ocular inflammatory disorders: recommendations of an expert panel. *Am J Ophthalmol*. 2000;130(4):492–513.
3. Kempen JH, Daniel E, Dunn JP, et al. Overall and cancer related mortality among patients with ocular inflammation treated with immunosuppressive drugs: retrospective cohort study. *BMJ*. 2009;339:b2480.
4. Knickelbein JE, Kim M, Argon E, Nussenblatt RB, Sen NH. Comparative efficacy of steroid-sparing therapies for noninfectious uveitis. *Expert Rev Ophthalmol*. 2017;12(4):313–319.
5. Visentin M, Zhao R, Goldman ID. The antifolates. *Hematol Oncol Clin North Am*. 2012;26(3):629–648.
6. Brown PM, Pratt AG, Isaacs JD. Mechanism of action of methotrexate in rheumatoid arthritis, and the search for biomarkers. *Nat Rev Rheumatol*. 2016;12(12):731–742.
7. Zandman-Goddard G, Shoenfeld Y. Mycophenolate mofetil in animal models of autoimmune disease. *Lupus*. 2005;14(Suppl 1):S12–S16.
8. Allison AC. Mechanisms of action of mycophenolate mofetil. *Lupus*. 2005;14(Suppl 1):S2–S8.
9. Ma W, Mao Q, Xia W, Dong G, Yu C, Jiang F. Gut Microbiota Shapes the Efficiency of Cancer Therapy. *Front Microbiol*. 2019;10:1050.
10. Sayers E, MacGregor A, Carding SR. Drug-microbiota interactions and treatment response: Relevance to rheumatoid arthritis. *AIMS Microbiol*. 2018;4(4):642–654.
11. Heissigerova J, Seidler Stangova P, Klimova A, et al. The Microbiota Determines Susceptibility to Experimental Autoimmune Uveoretinitis. *J Immunol Res*. 2016;2016:5065703.
12. Lin P. The role of the intestinal microbiome in ocular inflammatory disease. *Curr Opin Ophthalmol*. 2018;29(3):261–266.
13. Chanaud NP, Vistica BP, Eugui E, Nussenblatt RB, Allison AC, Gery I. Inhibition of experimental autoimmune uveoretinitis by mycophenolate mofetil, an inhibitor of purine metabolism. *Exp Eye Res*. 1995;61(4):429–434.
14. Hiraoka M, Mihara M, Takeda Y, Miyasaka N. A novel non-polyglutamable anti-folate, MX-68, inhibits the induction

of experimental autoimmune uveitis in rats. *Exp Eye Res*. 1998;67(1):1–8.

15. Caspi RR, Roberge FG, Chan CC, et al. A new model of autoimmune disease. Experimental autoimmune uveoretinitis induced in mice with two different retinal antigens. *J Immunol*. 1988;140(5):1490–1495.
16. Nakamura YK, Janowitz C, Metea C, et al. Short chain fatty acids ameliorate immune-mediated uveitis partially by altering migration of lymphocytes from the intestine. *Sci Rep*. 2017;7(1):11745.
17. Agarwal RK, Caspi RR. Rodent models of experimental autoimmune uveitis. *Methods Mol Med*. 2004;102:395–419.
18. Nakamura YK, Metea C, Karstens L, et al. Gut Microbial Alterations Associated With Protection From Autoimmune Uveitis. *Invest Ophthalmol Vis Sci*. 2016;57(8):3747–3758.
19. Gilbert JA, Meyer F, Jansson J, et al. The Earth Microbiome Project: Meeting report of the "1 EMP meeting on sample selection and acquisition" at Argonne National Laboratory October 6 2010. *Stand Genomic Sci*. 2010;3(3):249–253.
20. Callahan BJ, McMurdie PJ, Rosen MJ, Han AW, Johnson AJA, Holmes SP. DADA2: High-resolution sample inference from Illumina amplicon data. *Nat Methods*. 2016;13(7):581–583.
21. McMurdie PJ, phyloseq Holmes S.: An R Package for Reproducible Interactive Analysis and Graphics of Microbiome Census Data. *PLoS One*. 2013;8(4):e61217.
22. Wright ES. Using DECIPHER v2.0 to Analyze Big Biological Sequence Data in R. *The R Journal*. 2016;8(1):352–359.
23. Love MI, Huber W, Anders S. Moderated estimation of fold change and dispersion for RNA-seq data with DESeq2. *Genome Biol*. 2014;15(12):550.
24. Schneider CA, Rasband WS, Eliceiri KW. NIH Image to ImageJ: 25 years of image analysis. *Nat Methods*. 2012;9(7):671–675.
25. Rubio CA, Schmidt PT, Lang-Schwarz C, Vieth M. Branching crypts in inflammatory bowel disease revisited. *J Gastroenterol Hepatol*. 2021;37:440–445.
26. Nouri M, Bredberg A, Weström B, Lavasani S. Intestinal barrier dysfunction develops at the onset of experimental autoimmune encephalomyelitis and can be induced by adoptive transfer of auto-reactive T cells. *PLoS One*. 2014;9(9):e106335.
27. Hoffmann W, Jagla W, Wiede A. Molecular medicine of TFF-peptides: from gut to brain. *Histol Histopathol*. 2001;16(1):319–334.
28. Thornton AM, Shevach EM. Helios: still behind the clouds. *Immunology*. 2019;158(3):161–170.
29. Seng A, Krausz KL, Pei D, et al. Coexpression of FOXP3 and a Helios isoform enhances the effectiveness of human engineered regulatory T cells. *Blood Adv*. 2020;4(7):1325–1339.
30. Long Y, Zhao X, Xia C, Liu X, Fan C, Liu C. Infection of Epstein-Barr Virus is Associated with the Decrease of Helios(+)FoxP3(+)Regulatory T Cells in Active Ulcerative Colitis Patients. *Immunol Invest*. 2021;50(1):23–36.
31. Duncan SH, Barcenilla A, Stewart CS, Pryde SE, Flint HJ. Acetate utilization and butyryl coenzyme A (CoA): acetate-CoA transferase in butyrate producing bacteria from the human large intestine. *Appl Environ Microbiol*. 2002;68(10):5186–5190.
32. Li H, Liu F, Lu J, et al. Probiotic Mixture of Lactobacillus plantarum Strains Improves Lipid Metabolism and Gut Microbiota Structure in High Fat Diet-Fed Mice. *Front Microbiol*. 2020;11:512.
33. Zhao L, Zhang Q, Ma W, Tian F, Shen H, Zhou M. A combination of quercetin and resveratrol reduces obesity in high-fat diet-fed rats by modulation of gut microbiota. *Food Funct*. 2017;8(12):4644–4656.
34. Zhu J, Kong Y, Yu J, et al. Consumption of drinking water N-Nitrosamines mixture alters gut microbiome and increases the obesity risk in young male rats. *Environ Pollut*. 2019;248:388–396.
35. Keishi K, Kikuji I. Intestinal colonization by a Lachnospiraceae bacterium contributes to the development of diabetes in obese mice. *Microbes Environ*. 2014;29(4):427–430.
36. Meehan CJ, Beiko RG. A phylogenomic view of ecological specialization in the lachnospiraceae, a family of digestive tract-associated bacteria. *Genome Biol Evol*. 2014;6(3):703–713.
37. Janowitz C, Nakamura YK, Metea C, et al. Disruption of Intestinal Homeostasis and Intestinal Microbiota During Experimental Autoimmune Uveitis. *Invest Ophthalmol Vis Sci*. 2019;60(1):420–429.
38. Xu Y, Wang N, Tan HY, Li S, Zhang C, Feng Y. Function of Akkermansia muciniphila in Obesity: Interactions With Lipid Metabolism, Immune Response and Gut Systems. *Front Microbiol*. 2020;11:219.
39. Earley H, Lennon G, Balfe A, Coffey JC, Winter DC, O'Connell PR. The abundance of Akkermansia muciniphila and its relationship with sulphated colonic mucins in health and ulcerative colitis. *Sci Rep*. 2019;9(1):15683.
40. Zhang T, Li Q, Cheng L, Buch H, Zhang F. Akkermansia muciniphila is a promising probiotic. *Microb Biotechnol*. 2019;12(6):1109–1125.
41. Vacca M, Celano G, Calabrese FM, Portincasa P, Gobbetti M, De Angelis M. The Controversial Role of Human Gut Lachnospiraceae. *Microorganisms*. 2020;8(4):573.
42. Ma L, Ni Y, Wang Z, et al. Spermidine improves gut barrier integrity and gut microbiota function in diet-induced obese mice. *Gut Microbes*. 2020;12(1):1–19.
43. Hu S, Wang J, Xu Y, et al. Anti-inflammation effects of fucosylated chondroitin sulphate from Acaudina molpadioides by altering gut microbiota in obese mice. *Food Funct*. 2019;10(3):1736–1746.
44. Yasar Bilge NS, Pérez Brocal V, Kasifoglu T, et al. Intestinal microbiota composition of patients with Behçet's disease: differences between eye, mucocutaneous and vascular involvement. The Rheuma-BIOTA study. *Clin Exp Rheumatol*. 2020;38(Suppl. 5):60–68.
45. Li J, Wu T, Li N, Wang X, Chen G, Lyu X. Bilberry anthocyanin extract promotes intestinal barrier function and inhibits digestive enzyme activity by regulating the gut microbiota in aging rats. *Food Funct*. 2019;10(1):333–343.

Investigative Ophthalmology & Visual Science